International Journal of Aviation Science and Technology

Research Article

Design and Simulation of Seats for Emergency Landing Conditions in Electrical VTOLs

Hasan Totoş[1*], Çağlar Üçler[2]

[1] *Istanbul Technical University, Aviation Institute, Department of Defense Technologies, Istanbul, Turkiye*
hasantotos53@gmail.com - 0009-0001-1829-3046
[2] *Ozyegin University, Faculty of Aviation and Aeronautical Sciences, Istanbul, Turkiye*
caglar.ucler@ozyegin.edu.tr - 0000-0003-4209-7915

Abstract

Emerging electrification technologies in aviation and recent advances drive the increased usage of electrical vertical take-off and landing (VTOL) air vehicles. Weight considerations are predominant due to the weaker powertrain and lower payload capacity. Moreover, most systems are automated, and there is no distinction between pilot and passenger seats anymore. Conventional aircraft seating typically exhibits excessive weight, necessitating the development of lightweight troop seats with simple designs and textile seat pans and backrests. This research focuses primarily on the design aspects of these lightweight troop seats. There are already guiding military standards and civilian codes for physical tests for passenger or pilot seats. Nevertheless, there needs to be a comprehensive document combining all of these and explaining how simulation tools can be practically used for the same purpose. Consequently, a generic design was generated based on the troop seat of military helicopters, which was then tested and simulated virtually by finite element analysis according to MIL-S-85510, CS27, and CS29 standards. After finalizing the static tests for forward, rearward, lateral, downward, and upward g forces on a 10-degree floor deformation in the longitudinal axis, implicit dynamic tests were conducted with loading in longitudinal and vertical directions as specified by the MIL-S-85510 standards. Then, hotspot analysis is made for stress interpretation. As a result, a near-optimum design was achieved with stresses 10% lower than the yield stress of the materials, which can be used on board an electrical VTOL.

Keywords

VTOL
Seat
Design
Analysis
MIL-S-85510
CS27
CS29

Time Scale of Article

Received 14 February 2024
Revised until 15 May 2024
Accepted 17 May 2024
Online date 21 June 2024

1. Introduction

The aviation sector is rapidly growing (Alharasees et. al., 2023) and electrification technologies in transportation are rapidly transforming aviation. Vertical take-off and landing (VTOL) air vehicles are becoming popular, and their penetration is further boosted by the mission flexibility provided (Aldemir and Ucler, 2022). Since VTOLs can take off and land vertically, they are an ideal candidate for military usage and civil applications when no runway is available (Zhou et al, 2020). In some missions, VTOLs are necessary to track objects or make stationary measurements when hovering (Ozdemir et al., 2014). Moreover, there is a broad application of VTOLs in observation for military purposes, transport of cargo, and rescuing soldiers and victims (Intwala and Parikh, 2015). In addition to these, they can be used for security

*: Corresponding Author Hasan Totoş, hasantotos53@gmail.com
DOI: 10.23890/IJAST.vm05is01.0101

operations, climate examination, and forest fire detection (Dinç, A., 2020).

Nevertheless, the structural requirements for VTOLs are very high. There are two distinct ways of designing them; either military or civilian codes can be used. In civil aviation, helicopter standards must be respected. For military VTOL cockpit seats, the MIL-S-58095 standard is used (DoD, 1981). For cabin seats, MIL-S-85510 is used (DoD, 1981). Nevertheless, the new generation VTOLs are highly automated, and there is no distinction between passenger and pilot seats anymore. Considering that the g levels for cabin seats are lower than cockpit seats (Demircan, 2020), but regular pilot seats are too heavy for a weaker electrical powertrain, troop seats can be used for electrical VTOLs. Moreover, civil aviation codes CS27 and CS29 standards must be respected as well (EASA, 2018; EASA 2018).

Historically, there have been some accidents in which humans get injured because of troop seat's insufficient strength (Reilly, 1977). The structural strength of the seats is a vital factor for protecting the occupant in crash events. Aviation standards contain various guidelines and criteria to ensure that seats meet specific minimum structural strength requirements, where static loads and peak acceleration values are defined for physical tests.

This study aims to improve the structural strength of the troop seat for electrical VTOLs by utilizing simulation technologies. In a crash, the design must be strong enough to withstand the loads without breaking, and the permanent deformation must absorb the energy. This requires an optimum design with appropriate materials selected. Current seat designs need to be improved to increase their impact-damping capabilities and optimized to protect inmates in the event of a crash.

Consequently, the research questions are:

- RQ 1: Which boundary conditions and loads can be used to develop a cheap, lightweight, and strong troop seat for electrical VTOLs?
- RQ 2: What is a near-optimum design for a certification-ready electrical VTOL?

This research investigates different material selections and structural design variations made by the SolidWorks program with virtual simulations by the ANSYS program. First, a literature review was leveraged to isolate the calculation, i.e., simulation basis. Then, the method is explained in detail, where the initial design was made according to MIL-S-85510 standard with a mixed model of shell and solid elements to reduce the computational time, which was optimized after applying g loads with the maximum values across MIL-S-85510, CS27, and CS29 standards. The discussion uses mesh sensitivity analysis and successive hotspot analysis for high-stress regions in an iterative manner.

It has been shown that the structural strength of the troop seat can be increased by using different material combinations, and it was seen that some parts' thickness can be reduced to decrease the weight. This research has provided new design recommendations to increase the structural strength of seats and offered practical application recommendations for the aviation industry and troop seat manufacturers. Suggestions have been made as to what material combinations or design changes could increase the strength of troop seats without increasing the weight and manufacturing costs.

2. Literature review

Amaze et. Al. (2024) studied commercial aircraft seat support structure analysis and topology optimization. Design and analysis conducted by the Solidworks program. Al6061-TS6(SS), Al7075-T6(SN),1023Carbon steel sheet (SS) and KYDEX®T materials were used. After topology optimization, the maximum stress observed was 189 MPa, and weight was reduced by 30% to 1.89 kg. Weight reduction achieved without loss of necessary strength.

Trivers et al. (2020) studied business aircraft seat design by topology optimization. In this study, Canadian Aviation Regulations 525.561 and 525.562 parts were used for making static and dynamic tests. Two topology optimizations were made for decreasing the manufacturing costs and decreasing the weight. They use explicit dynamic models to determine the response of the seat under 14g and 16g. 77.11 kg is used as an occupant. The static ultimate load factors are 9 g for forward, 4 g for sideward, 3 g for upward, 6 g for downward, and 1.5 g for rearward. 2024 T351 aluminum was used for the preliminary design. Buckling and complete fractures were unacceptable. But, the small amount of harm and yielding is not considered a problem for the design. However, there are some limitations of that study, the floor deformation was not considered in the analysis, and due to the limited density of meshes, results are approximately close to real cases. The results showed that the weight of the seat must be 32% lighter and the manufacturing costs decreased by 24%.

Tzanakis et al. (2023) researched composite aircraft seat structural analysis. In this study, Part 25.561 and 25.562 guidelines were used. According to the 25.562 guidelines, two dynamic tests are made. One with 14g and the other one with 16 g. Economy class 3 people seat is used. Von Misses' stress evaluation showed that the front seat rows were subjected to more loadings than the back rows due to the passenger's impact. Results showed that there is no significant material damage or critical loads on the structure. Injury criteria were also investigated with LS-DYNA software.

Özturk and Kayran (2018) studied crash analysis and the energy absorption mechanism of helicopter seats. EASA standards are used. The ABAQUS program is used for analysis. In this study, the seat hit a fixed wall, and the seat deformation was investigated. The tests were made with and without absorbers. The seat legs were aluminum. The g loads of seat and EASA standards compared to conclude that the seat is crashworthy. The effectiveness of the energy absorption mechanism is investigated.

3. Method

In crash events, the fuselage and cabin will be deformed (Trivers et al, 2020). The aircraft floor should be deformed so that this floor warpage conditions are also considered before and throughout tests (DoD,1981). One of the floor attachments of the floor-connected seats should be misaligned 10 degrees in pitch, and the other floor attachment of the seat should be misaligned 10 degrees in roll (Wiggenraad,1997). For tests, the maximum g values of the CS27/29 and MIL-S-85510 standards were used in the analysis. For the forward static test, 30 g, rearward test, 12 g, lateral test, 23 g, and upward test, 8 g load was applied according to MIL-S-85510 standards. For the downward test, 20 g was applied. CS 27/29 standards were considered in the downward test because the load requirement was higher for the downward test in CS 27/29 standards. According to the CS 27/29 standards, the test should be 3 seconds. For other static tests, the time was taken as 1 second. For the vertical dynamic test, the minimum peak deceleration was 32 g at 0,087th second, and the maximum peak deceleration was 37 g at 0,059th second. For the longitudinal dynamic test, the minimum peak deceleration was 22 g at 0,127th second, and the maximum peak deceleration was 27 g at 0,0811th second.

The directions were considered for dynamic tests as shown in Figure 1 according to MIL-S-85510 standards. Test 1 configuration is for the vertical dynamic test, and test 2 configuration is for the longitudinal dynamic test in Figure 1. The dummy was taken as 110 kg for all tests except for downward static and vertical dynamic tests. For the downward static test dummy was taken as 75 kg according to the CS 27/29 standards and for the vertical dynamic test dummy was taken as 89 kg according to MIL-S-85510 standards.

Solidworks program was used for the CAD design. For analysis, Ansys software was used. The static structural module of the Ansys software was used for static tests. The transient structural module of the Ansys software was used for dynamic tests.

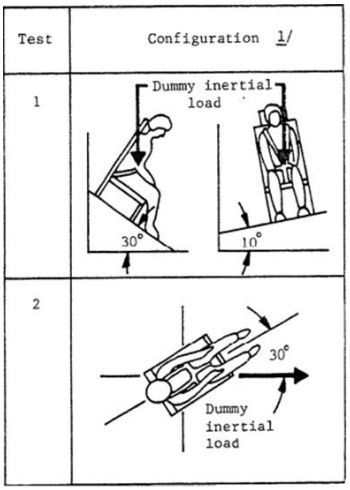

Fig. 1: Dynamic test conditions (DoD, 1981).

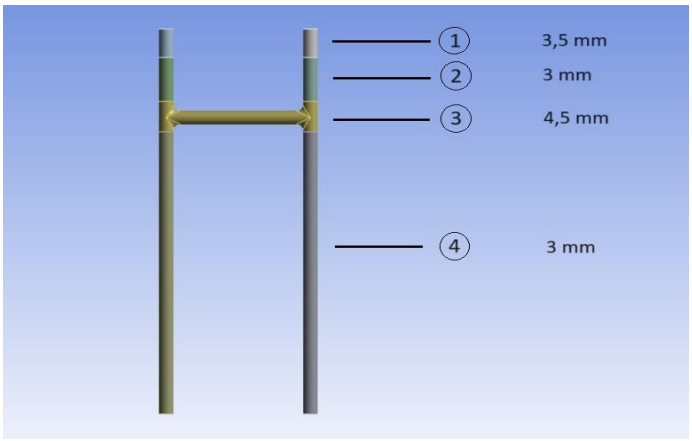

Fig. 2: Seat Pole design.

The seat pan, seat pole, seat belt, and fabrics were converted to shell models in SpaceClaim software for better mesh quality and faster analysis. The seat pole design is shown in Figure 2. For the upper leg of the seat pole, a thickness of 3,5 mm was used, labeled as 1 in Figure 2. High stress was observed on the upper leg of the seat pole. To reduce this, thickness increased. For the middle tube of the seat pole, a thickness of 4,5 mm was used, labeled as 3 in Figure 2. It was also because high stress was observed in the middle tube. For the rest of the seat pole, 3 mm thickness was appropriate, labeled as 2 and 4 in Figure 2.

The seat pan design is shown in Figure 3. Initially, the seat pan was 3 mm thick, but the thickness decreased to reduce the weight. For the 1st section, 2,5 mm thickness and for the 2nd section, 2 mm thickness was used as shown in Figure 3. A generic dummy model made of wood includes the passenger's weight, which is used in simplified real tests. The design is shown in Figure 4.

Different designs were tried to decrease the stress on the junction part. The flat junction part decreased the stresses, but a flat surfaced junction part would not be weldable; therefore, it could not be used. Increasing the area of the junction part was also tried, but the stresses were not changed.

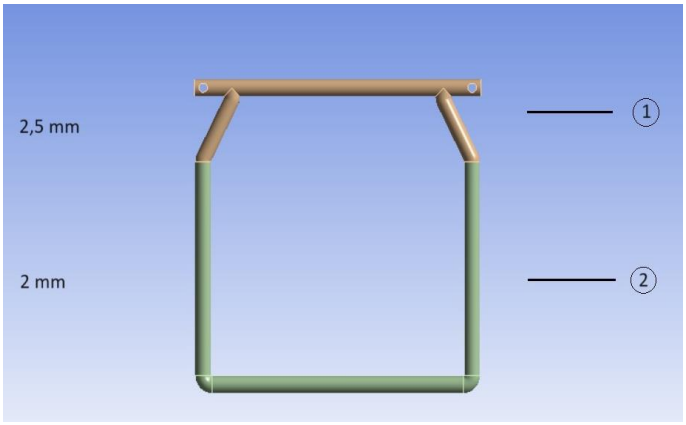

Fig. 3: Seat Pan design.

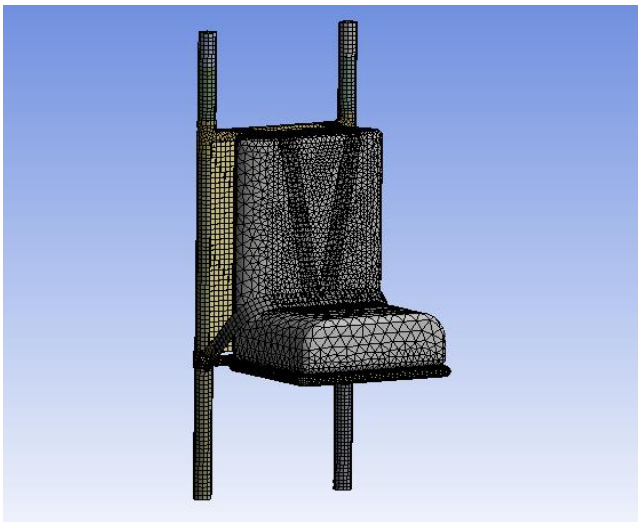

Fig. 4: Seat design.

Aluminum (Al) 7068 was used for the seat pole. For the seat pan, bolts, washers, and seatbelt buckle Al 7075 was used. For washers inside the junction part, copper alloy material was used, and for the junction part, solution-treated and aged Ti-8V-5Fe-1Al material was used. Seatbelts, seatbelt buckles, and fabrics were taken readily from ETSO standards, and the stress values on these parts were not investigated in this study. The weight limit was 6.8 kg according to MIL-S-85510 standards. The total weight of our design was 6,72 kg.

Finite element analysis (FEA) is a popular program used worldwide. Very complex problems can be solved by FEA (Roylance, 2001). FEA can make dynamic and static analyses. Static analysis is made to examine the fixed system's limits of force in the elastic region. Static analysis is a linear analysis method. Dynamic analysis is a nonlinear analysis type.

Dynamic analysis is a time-dependent analysis, and it considers the inertia effect (Balaban and Penekli, 2020). Dynamic analysis finds the dynamic behavior of the system. It is a widely known method; hence it is not explained in detail. Books written by Bhavikatti (2005) and Balaban and Penekli (2020) are good sources for further information.

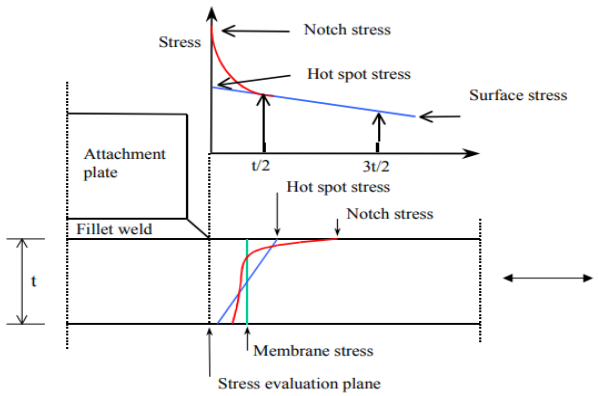

Fig. 5: Schematic stress distribution at a hotspot (DNV, 2011).

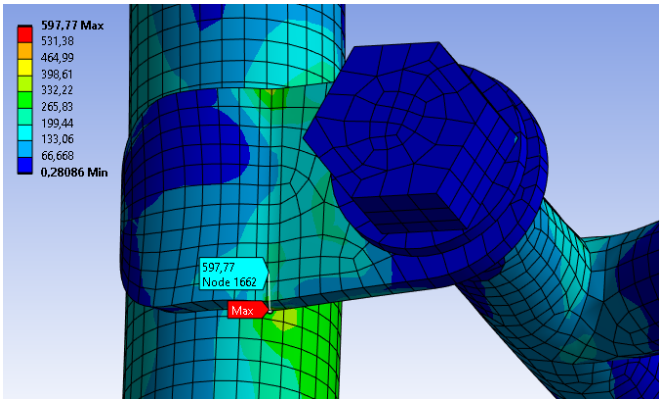

Fig. 6: Mesh sensitivity analysis for forward test.

Hotspot analyses were performed for high-stress values. This method is usually used for fatigue tests and determining actual stresses. It is used to find the actual stresses of the singularities and discontinuities. This stress is calculated with specific locations around the hotspot point (Caccese, 2010). The points with distances 0.5 t and 1.5 t from the hotspot point are used for extrapolation, where t represents the object's thickness (DNV, 2011). Stress distribution for hot spot analysis is shown in Figure 5.

4. Results and Discussion

Test 1: 30 g forward static test

The maximum stress was observed on the junction part for the forward static test. There was 577,22 MPa stress on the junction part. With a 5 mm element size, this stress increased to 597,77 MPa as shown in Figure 6. Then, hotspot analysis was made to investigate the real stress value. The stress at the point 2.5 mm away from the hotspot point was 386,4 MPa, and 7.5 mm away from the hotspot point was 214,65 MPa, as shown in Figure 7. With interpolation, hotspot analysis 1 showed that this stress was 472,275 MPa. Therefore, this stress value was considered as a singularity point.

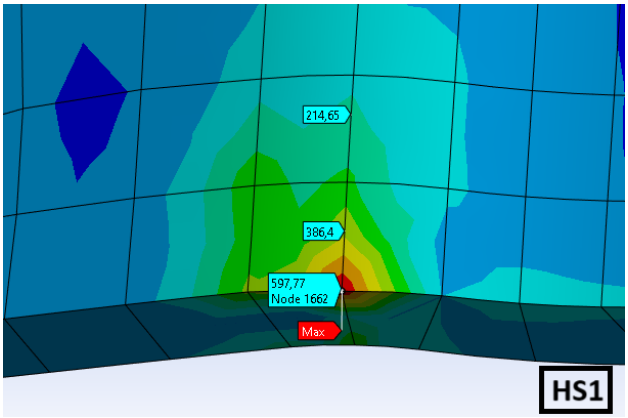

Fig. 7: Hotspot analysis 1 for forward test.

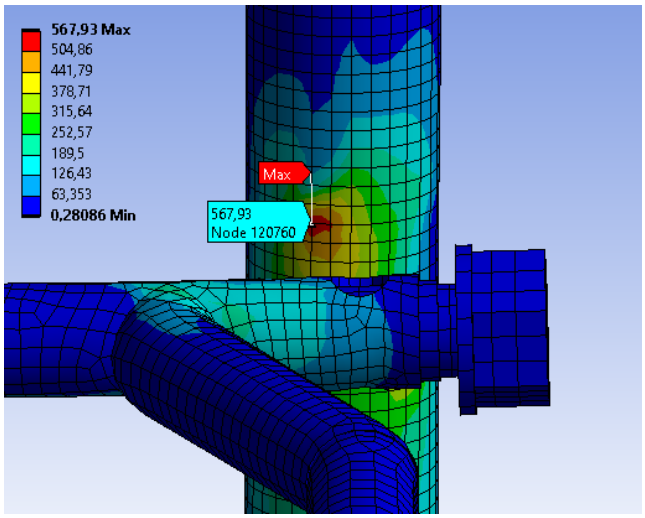

Fig. 8: Mesh sensitivity analysis for the main structure except the junction part.

Except for the junction part, the maximum stress was observed on the seat pole as 476,59 MPa. This stress increased to 567,93 MPa with mesh sensitivity analysis, as shown in Figure 8. Then, hotspot analysis 2 was made. At 0,5t away from the hotspot, the stress was 552,62 MPa; at 1,5t away from the hotspot, the stress was 522,11 MPa, as shown in Figure 9. By extrapolation, hotspot stress was found to be 567,875 MPa, almost the same as the stress value found by Ansys analysis. This means that this stress was not a singularity.

For the seat pan, the maximum stress observed was 259,84 MPa. This stress value decreased to 246,77 MPa with mesh sensitivity analysis, as shown in Figure 10. For the seat pan, 2,5 mm and 2 mm tubes were used. The maximum stress for copper alloy washers was 46,87 MPa, for bolts 118,83 MPa, and for washers 61,885 MPa. Hotspot analysis was not required for seat pans, bolts, washers, and copper alloy washers because the stresses were low.

All stresses on the forward static test were 10% lower than the yield strength of the materials, therefore this design was considered safe for the forward static test. The stresses observed on the forward static test are shown in Table 1.

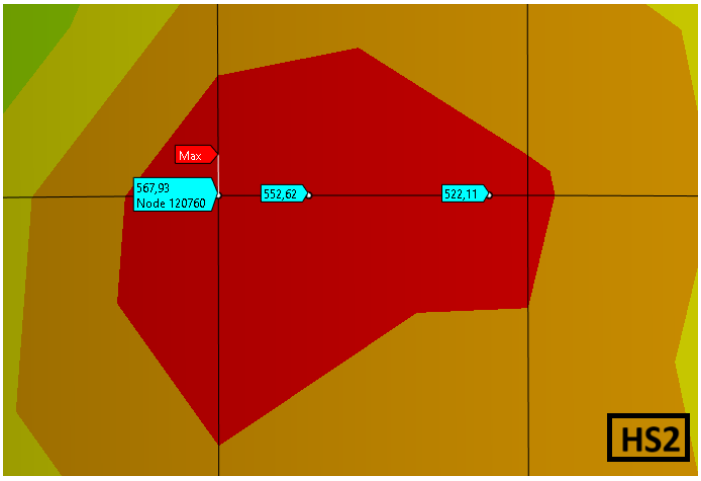

Fig. 9: Hotspot analysis HS2 for the forward test.

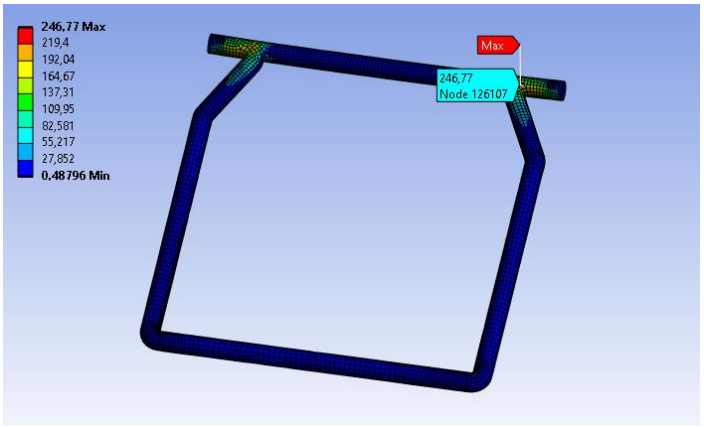

Fig. 10: Mesh sensitivity analysis for the seat pan.

Test 2: 12 g rearward static test

The maximum stress observed for the rearward static test was 226,81 MPa on the seat pole. With mesh sensitivity analysis, this stress increased to 314,65 MPa, as shown in Figure 11. Initially, Al 7034 material was used on the seat pole. But Al 7034 was not produced as a tube commonly. Therefore, Al 7068 was used on the seat pole, and it was seen that this material has enough strength for this part.

For the seat pan, the maximum stress observed was 95,258 MPa, as shown in Figure 12. Al 7075 was used on the seat pan, and Al 7075 material's yield stress was 503 MPa. 10% below the yield strength of Al 7075 was 452,7 MPa. 95,258 MPa was lower than 452,7 MPa. Therefore, mesh sensitivity analysis and hotspot analysis were not required.

The maximum stress observed for copper alloy washers was 6,6565 MPa, for bolts 38,6844 MPa, and for washers 9,7124 MPa. These stresses were 10% below the yield strength of the materials. Thus, this test passed the requirements without plastic deformation. The stress values observed on the rearward static test are shown in Table 2.

Table 1: Stress values for forward static test.

Forward Static Test	Materials	Stress (MPa)	Hotspot Analysis (MPa)	10% below the yield strength of the materials (MPa)
Junction Part	Ti-8V-5Fe-1Al (STA)	597,77	472,275	1242
Seat Pole	Al 7068	567,93	567,875	614,7
Seat Pan	Al 7075	246,77	NA*	452,7
Bolt	Al 7075	118,83	NA*	452,7
Copper Alloy Washer	Copper Alloy	46,87	NA*	252
Washer	Al 7075	61,885	NA*	452,7

NA*: Not available

Table 2: Stress values for rearward static test.

Rearward Static Test	Materials	Stress (MPa)	Hotspot Analysis (MPa)	10% below the yield strength of the materials (MPa)
Junction Part	Ti-8V-5Fe-1Al (STA)	130,47	NA*	1242
Seat Pole	Al 7068	314,65	NA*	614,7
Seat Pan	Al 7075	95,258	NA*	452,7
Bolt	Al 7075	38,684	NA*	452,7
Copper Alloy Washer	Copper Alloy	6,6565	NA*	252
Washer	Al 7075	9,7124	NA*	452,7

NA*: Not available

Test 3: 23 g lateral static test

The maximum stress observed for the 23 g lateral static test was 556,55 MPa on the junction part. This stress increased to 632,23 MPa with mesh sensitivity analysis, as shown in Figure 13. Then, hotspot analysis 3 was conducted to assess this stress. 0,5t away from the hotspot, there was 578,43 MPa stress; 1,5t away from the hotspot, there was 457,19 MPa stress, as shown in Figure 14. Extrapolated stress was 639,05 MPa. The hotspot stress increased from 632,23 MPa to 639,05 MPa. Therefore, 632,23 MPa was considered as a true stress.

Except for the junction part, the maximum stress was 432,48 MPa observed on the seat pole, as shown in Figure 15. Initially, 3 mm thick tubes were used on the seat pole's upper legs. However, it was seen that 3 mm tubes do not have enough strength. Thus, to decrease the stresses on the seat pole's upper legs, 3,5 mm thick tubes were used. Then, mesh sensitivity analysis was made with a 5 mm element size for this region. The 432,48 MPa stress increased to 493,65 MPa with mesh sensitivity analysis on the seat pole's upper leg, as shown in Figure 16. Hotspot analysis 4 made to this stress. With hotspot analysis, this stress was found to be 493,625 MPa, almost the same as that found by the analysis. Therefore, this stress value was a real stress.

On the seat pole's middle tube, 4,5 mm thickness was used. In the earlier design, 3 mm thickness was used. It was seen that there were high-stress values with 3 mm thickness. Hence thickness increased to 4,5 mm. Thus, stress values decreased. Making a mesh sensitivity analysis with a 5 mm element size to that region to get a more accurate stress value. It is obtained that 482,94 MPa stress occurred in this region with mesh sensitivity analysis as shown in Figure 17.

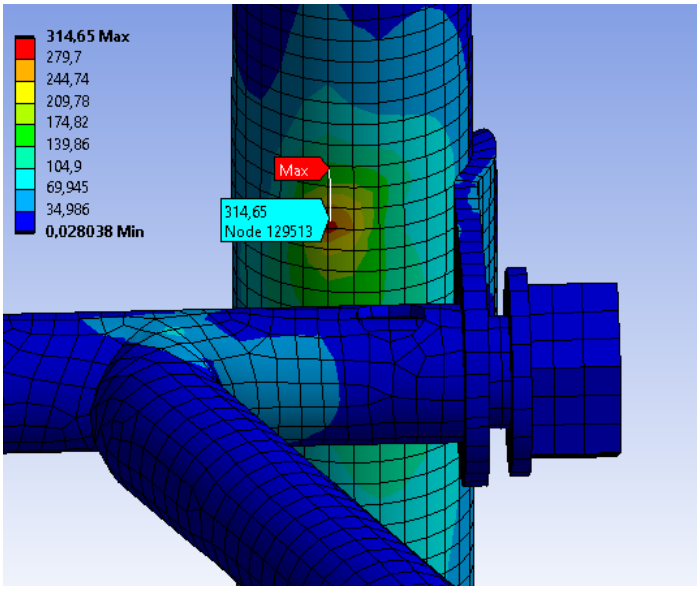

Fig. 11: Mesh sensitivity analysis for rearward test.

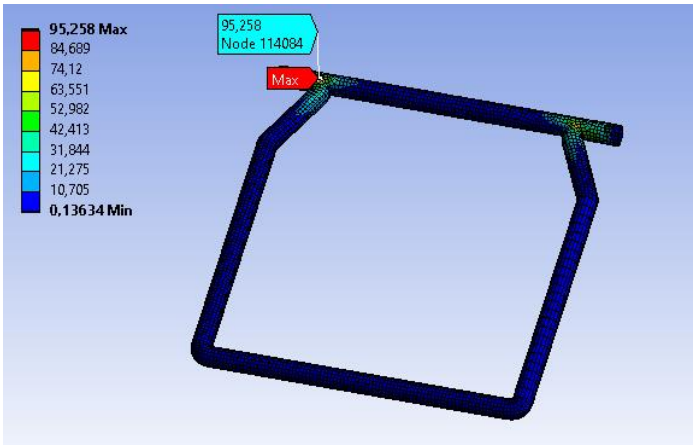

Fig. 12: Seat Pan analysis for rearward test.

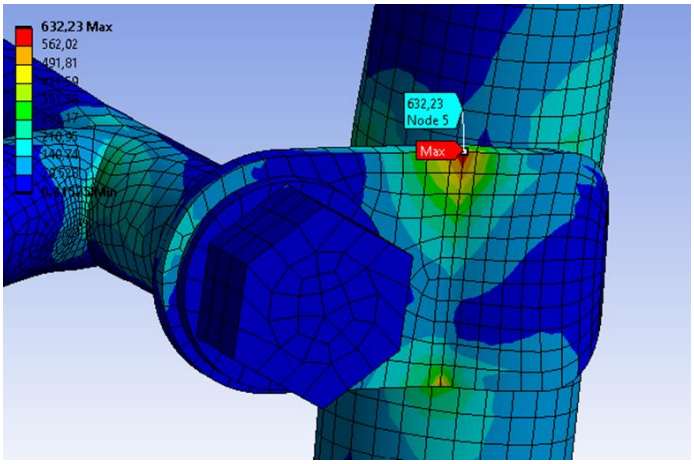

Fig. 13: Mesh sensitivity analysis for the lateral test.

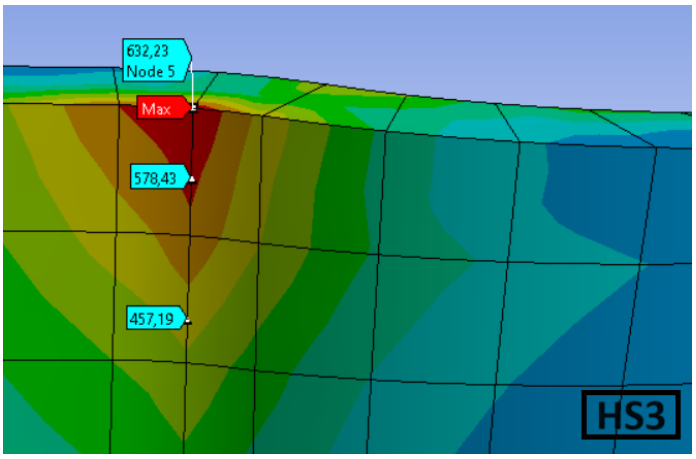

Fig. 14: Hotspot analysis 3 (HS3) for the lateral test.

Hotspot analysis 5 was made to find the actual stress for 482,94 MPa stress. The hotspot stress increased from 482,94 MPa to 499,725 MPa. These stresses were still lower than the 614,7 MPa critical stress value for the Al 7068 material. Therefore, this stress value was not dangerous.

The maximum stress on the seat pan observed was 357,76 MPa. To investigate it better a mesh sensitivity analysis was made with a 5 mm element size and the stress increased to 416,98 MPa as shown in Figure 18.

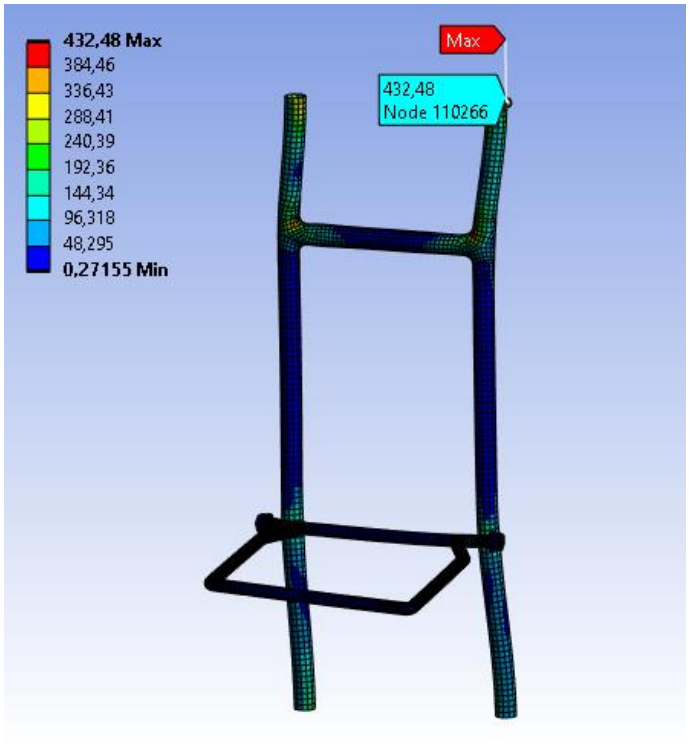

Fig. 15: Maximum stress on the main structure except the junction part for the lateral test.

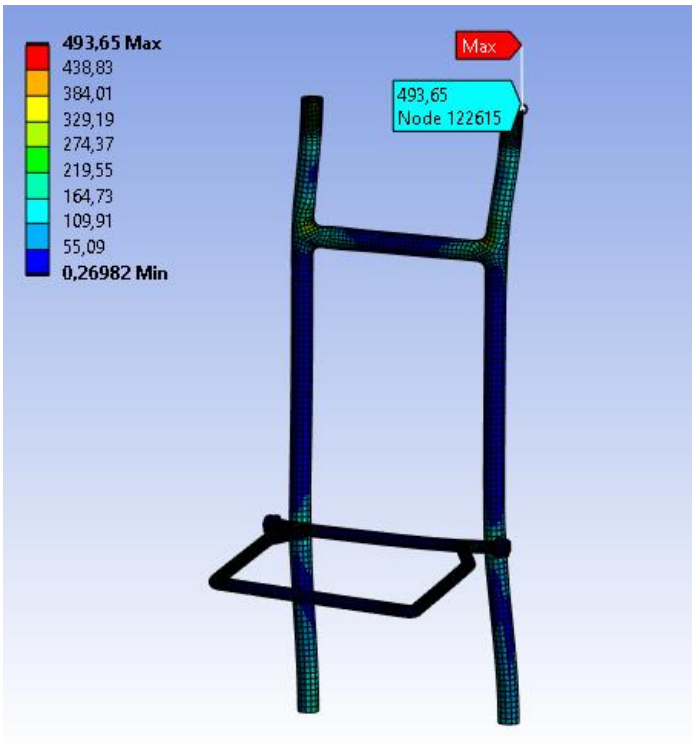

Fig. 16: Mesh sensitivity analysis of seat pole upper legs for the lateral test.

Since this stress was high, hotspot analysis 6 was performed on this stress. With hotspot analysis, this stress value was found to be 413,435 MPa. It was very close to the stress found by the analysis. 413,435 MPa was very low from the Al 7075 material's yield strength.

Table 3: Stress values for lateral static test.

Lateral Static Test	Materials	Stress (MPa)	Hotspot Analysis (MPa)	10% below the yield strength of the materials (MPa)
Junction Part	Ti-8V-5Fe-1Al (STA)	632,23	639,05	657
Seat Pole	Al 7068	493,65	493,625	614,7
Seat Pan	Al 7075	416,98	413,435	452,7
Bolt	Al 7075	176,32	NA*	452,7
Copper Alloy Washer	Copper Alloy	80,313	NA*	252
Washer	Al 7075	95,286	NA*	452,7

NA*: Not available

For the copper alloy washer, the maximum stress observed was 80,313 MPa. The maximum stress observed for the bolts was 176,32 MPa; for the washers, the maximum stress observed was 95,286 MPa. For the lateral test, it is concluded that these values are very below the material's yield strength. Therefore, there will be no plastic deformation in the structure. The stress results observed for the lateral static test are given in Table 3.

Test 4: 20 g downward static test

CS 27/29 standards were used for the downward static test because the load was higher in CS 27/29 standards and the analysis was made for 3 seconds according to the CS 27/29 standards. The maximum stress observed for the downward static test was 590,43 MPa on the junction part. Then, mesh sensitivity analysis was made, and this stress increased to 674,33 MPa, as shown in Figure 19.

For the junction part, hotspot analysis 7 was made. The hotspot stress was calculated as 626,975. Hotspot analysis showed that true stress decreased from 674,63 MPa to 626,975 MPa. This stress was a singularity stress. For the junction part, Ti-8V-5Fe-1Al (STA) material was used. The 10% below the yield strength value of the Ti-8V-5Fe-1Al (STA) material was 1242 MPa. Therefore 626,975 MPa was in the safe region.

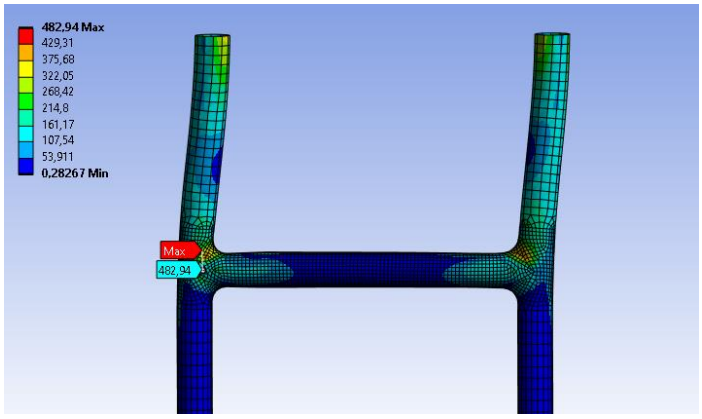

Fig. 17: Mesh sensitivity analysis for the middle tube for the lateral test.

If the stresses were investigated except the junction part, the maximum stress observed was 290,24 MPa on the seat pan. This stress decreased to 257,04 MPa with mesh sensitivity analysis, as shown in Figure 20.

Then to ensure that this stress value was real hotspot analysis 8 was made. The hotspot stress was calculated as 256,16 MPa. Hotspot analysis resulted in as same as the analysis made by Ansys. Thus, this stress value was real. This stress value was low for the Al 7075 material's yield strength. Therefore, no dangerous situation was observed.

The maximum stress for copper alloy washers was 59,754 MPa. For the bolt, the maximum stress was 109,22 MPa and for the washer, it was 59,048 MPa. Those stress values were very low. There won't be any plastic deformation occurrence on those parts. In summary, with analysis, it is ensured that there were no high-stress values for the downward test. This test passed the requirements of the CS27/CS29 standards. The stress results for the downward static test are shown in Table 4.

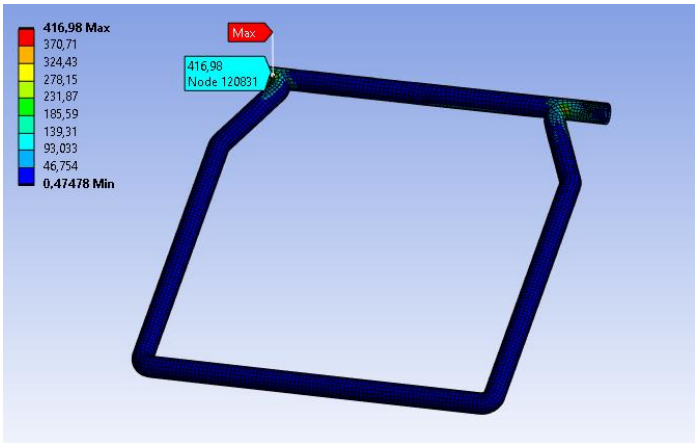

Fig. 18: Mesh sensitivity analysis for seat pan.

Table 4: Stress values for downward static test.

Downward Static Test	Materials	Stress (MPa)	Hotspot Analysis (MPa)	10% below the yield strength of the materials (MPa)
Junction Part	Ti-8V-5Fe-1Al (STA)	674,63	626,975	657
Seat Pole	Al 7068	220,64	NA*	614,7
Seat Pan	Al 7075	257,04	256,16	452,7
Bolt	Al 7075	109,22	NA*	452,7
Copper Alloy Washer	Copper Alloy	59,754	NA*	252
Washer	Al 7075	59,048	NA*	452,7

NA*: Not available

Test 5: 8 g upward static test

The maximum stress observed for the upward static test was 415,59 MPa on the junction part. With mesh sensitivity analysis, this stress decreased to 385,35 MPa. Hotspot analysis 9 made to this stress. With hotspot analysis, the stress was found to be 350,625 MPa. Hence, this stress value was a singularity stress.

The rest of the structure, except the junction part, was investigated, and the maximum stress was 112,58 MPa on the seat pole, as shown in Figure 21. This part of the seat pole was 3 mm thick. With 5 mm element size mesh sensitivity analysis, the 112,58 MPa stress increased to 206,09 MPa stress, as shown in Figure 22. Since Al 7068 material's yield strength was very high from this value. There was nothing to worry about. Hence, hotspot analysis wasn't required.

For the seat pan, the maximum stress observed was 81,002 MPa. To investigate the stress on the seat pan better, a mesh sensitivity analysis was performed on the seat pan with a 5 mm element size. With mesh sensitivity analysis, the maximum stress decreased to 74,682 MPa as shown in Figure 23. Al 7075 material was used on the seat pan. Since Al 7075 material's yield strength was 503 MPa and 10% below the yield strength was 452,7 MPa. 74,682 MPa stress value was low.

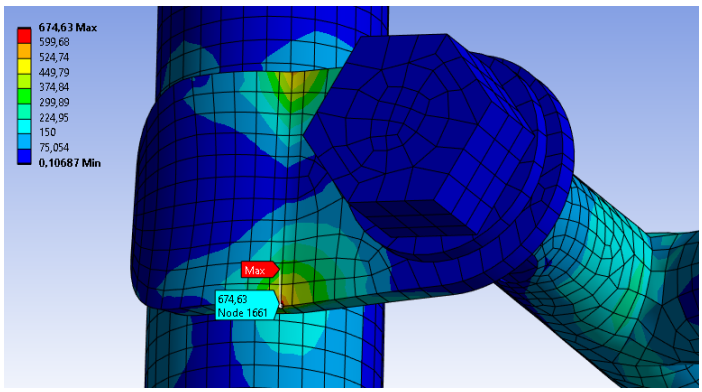

Fig. 19: Mesh sensitivity analysis for junction part.

For copper alloy washers, the maximum stress observed was 26,53 MPa. The maximum stress observed for the bolt was 34,773 MPa; for the washer, the maximum stress observed was 23,856 MPa. Since Al 7075 and copper alloy material's yield strength is very high from these stress values. There was no serious stress observation. In conclusion, stress values were low for the upward test, and it was ensured that this design is safe for the upward test without plastic deformation. The stress values observed for the upward static test are given in Table 5.

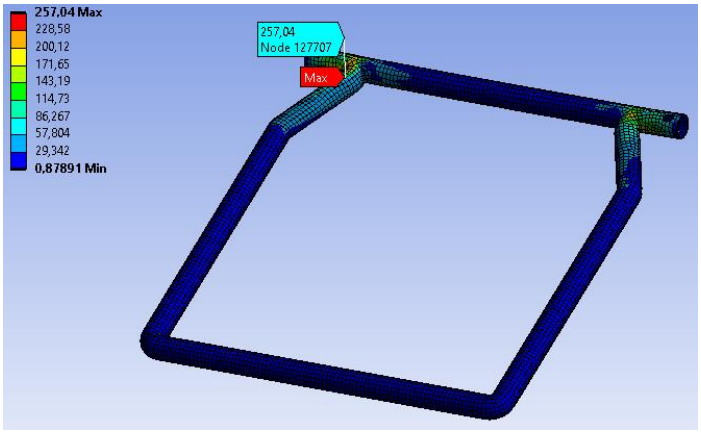

Fig. 20: Maximum stress on seat pan.

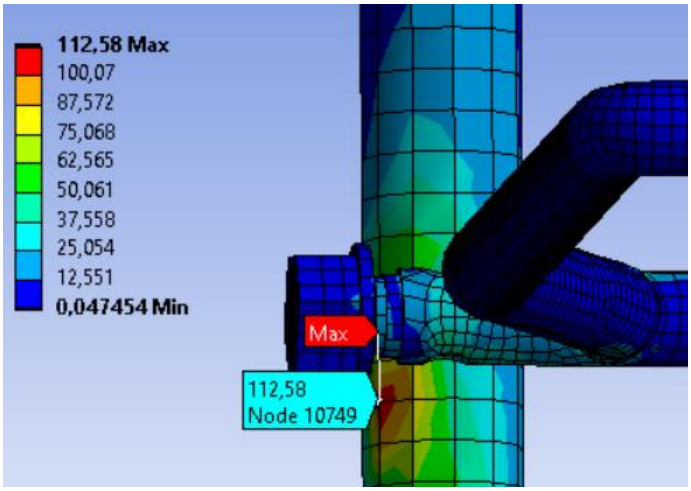

Fig. 21: Maximum stress except the junction part.

Table 5: Stress values for upward static test.

Upward Static Test	Materials	Stress (MPa)	Hotspot Analysis (MPa)	10% below the yield strength of the materials (MPa)
Junction Part	Ti-8V-5Fe-1Al (STA)	385,35	350,625	657
Seat Pole	Al 7068	206,09	NA*	614,7
Seat Pan	Al 7075	74,682	NA*	452,7
Bolt	Al 7075	34,773	NA*	452,7
Copper Alloy Washer	Copper Alloy	26,53	NA*	252
Washer	Al 7075	23,856	NA*	452,7

NA*: Not available

Test 6: 37g/32g vertical dynamic test

The maximum stress observed was 1331,8 MPa on the junction part for the vertical dynamic test at 0,05934th second. With mesh sensitivity analysis, this stress decreased to 1230 MPa at 0,05934th second. Hotspot analysis 10 was made for this stress region, and the stress was found to be 850,715 MPa with hotspot analysis. Hence this stress value was a singularity stress point. For the junction part, Ti-8V-5Fe-1Al (STA) material was used. 10% below this material's yield strength was 1242 MPa. 850,715 MPa was below the critical stress value.

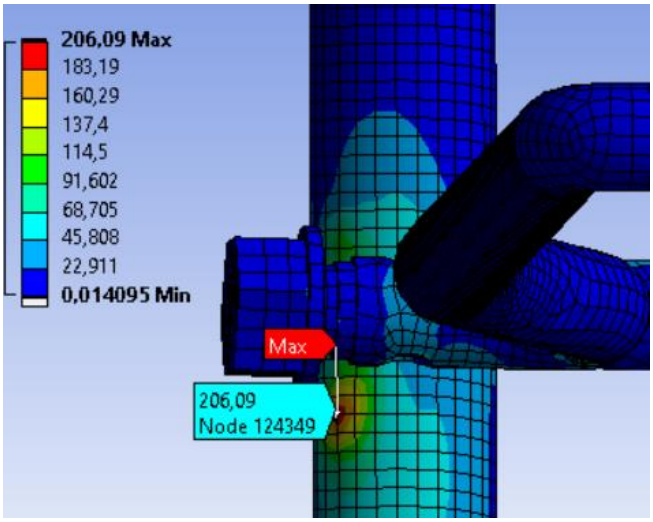

Fig. 22: Mesh sensitivity analysis of seat pole.

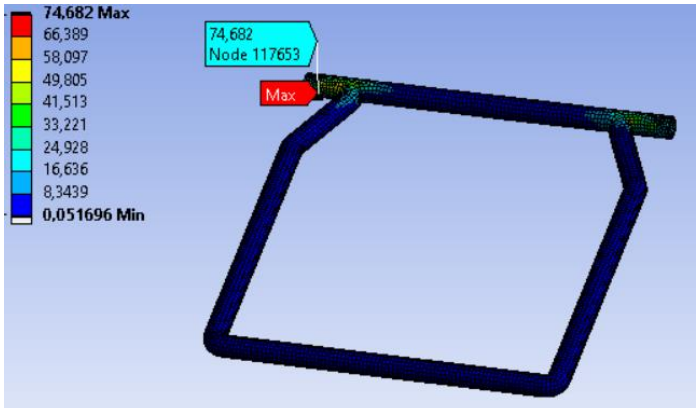

Fig. 23: Mesh sensitivity analysis of seat pan.

If we investigate the maximum stress except for the junction part. On the seat pole, 315,32 MPa stress was observed, as shown in Figure 24. With a 5 mm element size, mesh sensitivity analysis was made, and this stress increased to 520,29 MPa, as shown in Figure 25.

Hotspot analysis 11 made. This part of the seat pole was 3 mm. By making hotspot analysis, 520,135 MPa stress was observed. This stress was almost the same stress found by analysis.

The maximum stress on the seat pan observed was 226,55 MPa with a 5 mm element size, as shown in Figure 26. Initially, 3 mm tubes were used on the seat pan. Then, it was converted to 2,5 mm and 2 mm tubes for weight reduction. 226,55 MPa was a low stress; therefore, hotspot analysis was not required.

The maximum stress observed on the copper alloy washer was 71,847 MPa. For bolts, the maximum stress observed was 143,71 MPa; for washers, the maximum stress was 74,214 MPa. These were very low stresses. In conclusion, there were no stresses higher than 10 percent of the material's yield strengths for the vertical dynamic test. It is ensured that this design was safe for the vertical dynamic test. Stress results for vertical dynamic tests are shown in Table 6.

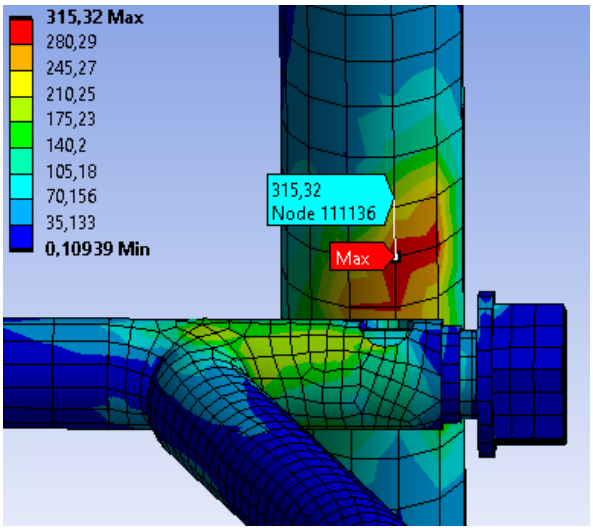

Fig. 24: Maximum stress except the junction part.

Table 6: Stress values for vertical dynamic test.

Vertical Dynamic Test	Materials	Stress (MPa)	Hotspot Analysis (MPa)	10% below the yield strength of the materials (MPa)
Junction Part	Ti-8V-5Fe-1Al (STA)	1230	850,715	657
Seat Pole	Al 7068	520,29	520,135	614,7
Seat Pan	Al 7075	226,55	NA*	452,7
Bolt	Al 7075	143,71	NA*	452,7
Copper Alloy Washer	Copper Alloy	71,847	NA*	252
Washer	Al 7075	74,214	NA*	452,7

NA*: Not available

Test 7: 27g/22g longitudinal dynamic test

For the longitudinal dynamic test, the maximum stress observed was 1008,8 MPa on the junction part at 0,081781th second. With mesh sensitivity analysis this stress decreased to 850,27 MPa at 0,087531th second as shown in Figure 27.

For the longitudinal dynamic test, hotspot analysis 12 was made for maximum stress on the junction part. The maximum stress was 850,27 MPa. The hotspot stress was calculated as 727,97 MPa. 850,27 MPa stress was found to be 727,97 MPa with hotspot analysis. It means that this stress was a singularity stress. Since 727,97 MPa was lower than the 1242 MPa, which was 10% below the Ti-8V-5Fe-1Al (STA) material's yield strength value. This stress was considered as safe.

If we investigate the maximum stress except for the junction part, high stress was observed on the seat pole. On that part of the seat pole, 3 mm thickness was used. 513,39 MPa stress was observed on the seat pole at 0,081781st second, as shown in Figure 28.

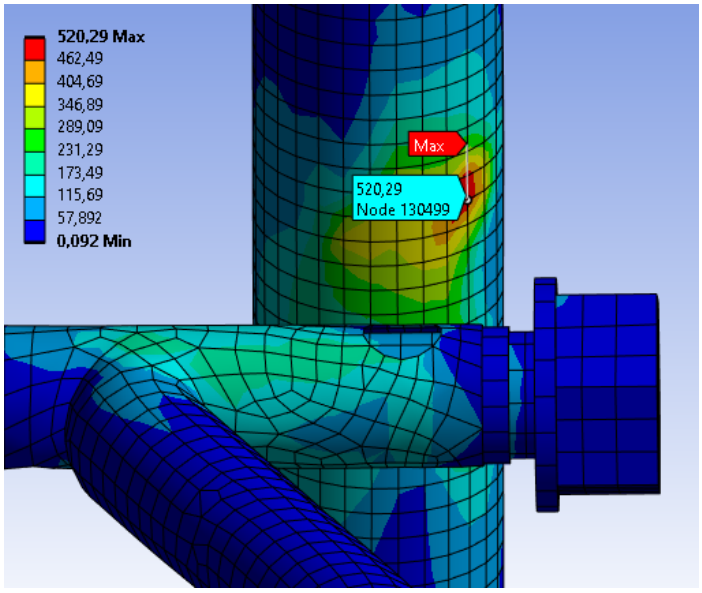

Fig. 25: Mesh sensitivity analysis of seat pole.

To investigate this stress better, a mesh sensitivity analysis was made with a 5 mm element size to this upper part of the seat leg. When a mesh sensitivity analysis was made. The 513,39 MPa stress value increased to 559,73 MPa at 0,087531st second, as shown in Figure 29.

559,73 MPa was a high-stress value. Therefore, hotspot analysis was performed to assess this stress. The hotspot stress was calculated as 559,65 MPa. Which was almost the same as 559,73 MPa stress. It was concluded that this stress was real stress.

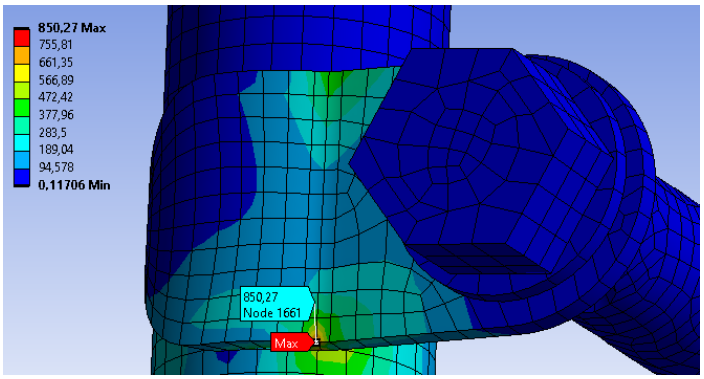

Fig. 26: Mesh sensitivity analysis for junction part.

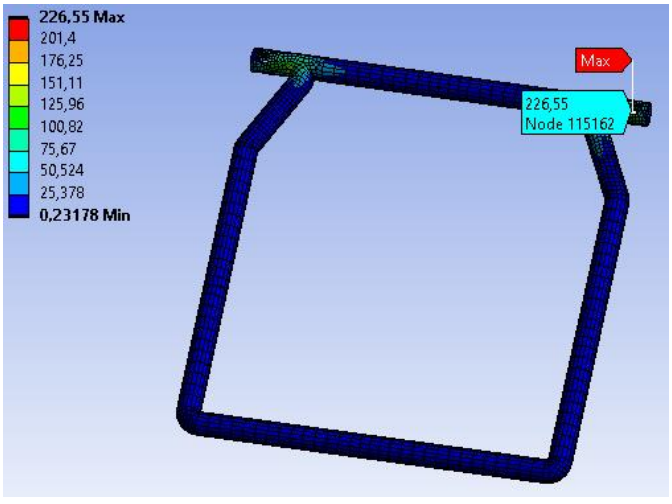

Fig. 27: Maximum stress on seat pan.

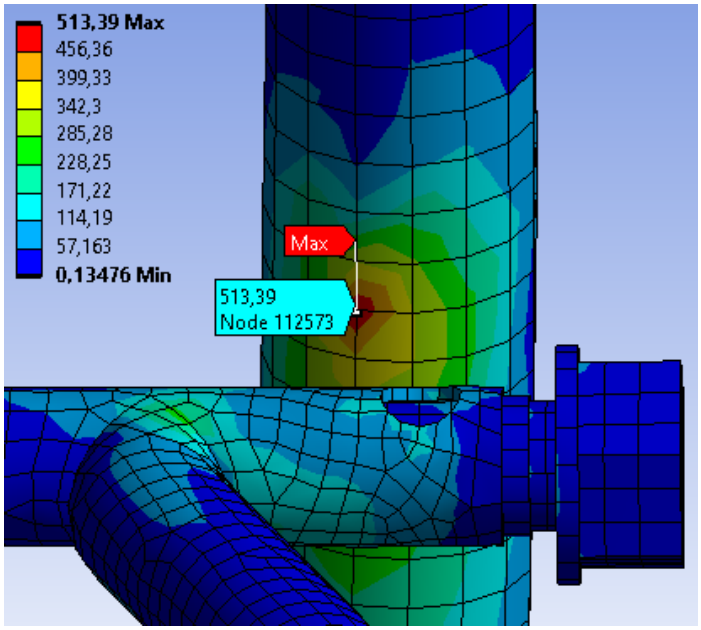

Fig. 28: Maximum stress except junction part.

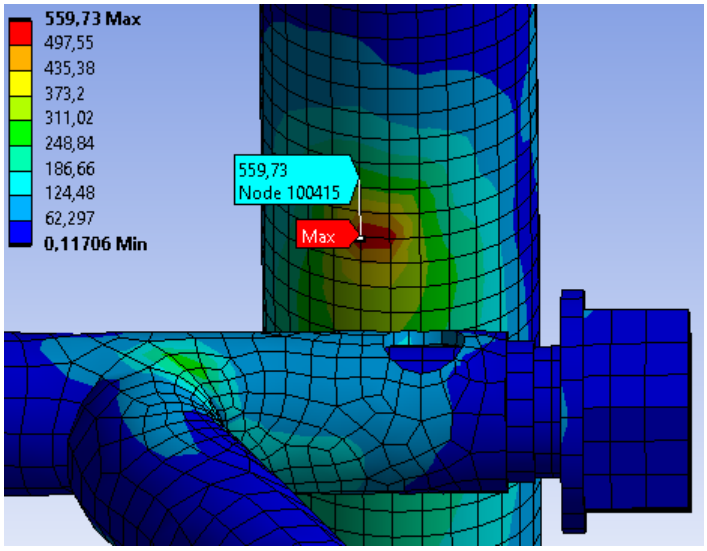

Fig. 29: Mesh sensitivity analysis of the seat pole.

Also, the upper legs of the seat pole were investigated for the longitudinal dynamic test with a 5 mm element size. A maximum of 522,31 MPa stress was observed on the upper leg of the seat pole, as shown in Figure 30. With hotspot analysis, this stress was found to be 522,075 MPa; it was ensured that this stress was real.

The maximum stress observed was 256,37 MPa on the seat pan at 0,085156th second with mesh sensitivity analysis as shown in Figure 31. The maximum stress observed on the copper alloy washer was 55,381 MPa at 0,081781th second. The maximum stress observed on bolts was 122,71 MPa, and the maximum stress observed for washers was 95,57 MPa. The stress results for the longitudinal static test are shown in Table 7.

Those findings show that instead of 3 mm, 2 and 2,5 mm parts can be used in the seat pan for weight reduction.

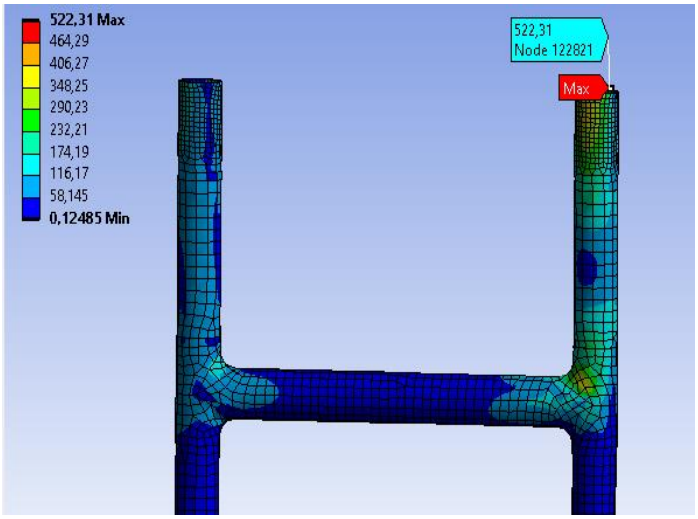

Fig. 30: Maximum stress on the upper legs.

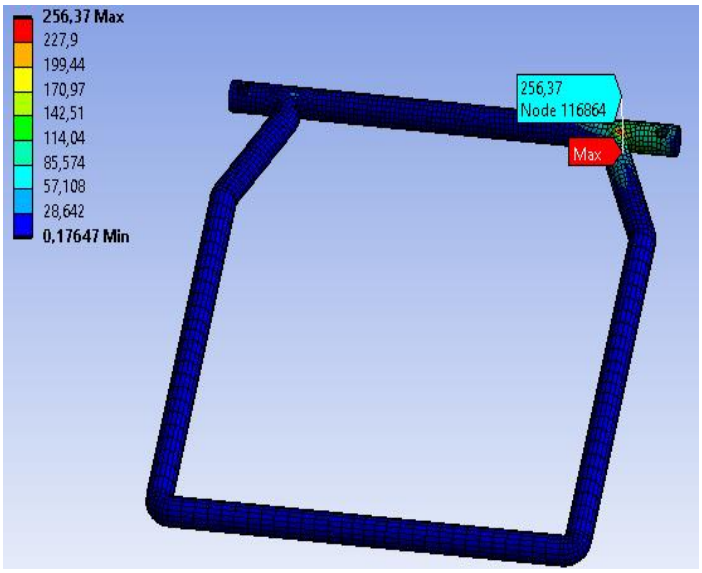

Fig. 31: Mesh sensitivity analysis of seat pan.

For the seat pole's middle tube, it was found that the 3 mm thickness was insufficient because high stress was observed in that part, especially in the lateral static test. Therefore, the thickness of the middle tube of the seat pole increased to 4,5 mm. For the upper leg of the seat pole, high stress was observed in the longitudinal dynamic test, and the thickness of this part increased to 3,5 mm. For the rest of the seat pole, 3 mm thickness was appropriate. In addition, in most tests, there was a singularity stress, which is an exaggerated stress result for the junction part. With hotspot analysis, it is shown that these stress results were lower.

Hotspot analysis showed that only 3 stress values occurred because of singularity in static tests. These singularities were on the junction part. For the junction part to decrease these singularity stresses, a flat junction part design was created, but since it was not weldable, it wasn't used. The hotspot analysis results are shown in Table 8.

Table 7: Stress values for longitudinal dynamic test.

Longitudinal Dynamic Test	Materials	Stress (MPa)	Hotspot Analysis (MPa)	10% below the yield strength of the materials (MPa)
Junction Part	Ti-8V-5Fe-1Al (STA)	850,27	727,97	657
Seat Pole	Al 7068	559,73	559,65	614,7
Seat Pan	Al 7075	256,37	NA*	452,7
Bolt	Al 7075	122,71	NA*	452,7
Copper Alloy Washer	Copper Alloy	55,381	NA*	252
Washer	Al 7075	95,57	NA*	452,7

NA*: Not available

Table 8: Hotspot analysis results for static tests.

Test	Hotspot	Maximum Stress (MPa)	Stress at t/2 (MPa)	Stress at 3t/2 (MPa)	Adjusted Hotspot Stress (MPa)
Forward static test	HS1	597,77	386,4	214,65	472,275 (Singularity)
	HS2	567,93	552,62	522,11	567,875
Lateral static test	HS3	632,23	578,43	457,19	639,05
	HS4	493,65	490,38	483,89	493,625
	HS5	482,94	475,38	426,69	499,725
	HS6	416,98	371,5	287,63	413,435
Downward static test	HS7	674,63	537,95	359,9	626,975 (Singularity)
	HS8	257,04	253,11	247,01	256,16
Upward static test	HS9	385,35	298,16	193,23	350,625 (Singularity)

Table 9: Hotspot analysis results for dynamic tests.

Test	Hotspot	Maximum Stress (MPa)	Stress at t/2 (MPa)	Stress at 3t/2 (MPa)	Adjusted Hotspot Stress (MPa)
Vertical dynamic test	HS10	1230	711,51	433,1	850,715 (Singularity)
	HS11	520,29	515,67	506,74	520,135
Longitudinal dynamic test	HS12	850,27	595,69	331,13	727,97 (Singularity)
	HS13	559,73	553,61	541,53	559,65
	HS14	522,31	518,95	512,7	522,075

In dynamic tests, all the stresses were below 10% of the yield stress of the materials. Hence, it was a safe design. 2 singularities were observed with hotspot analysis for dynamic tests. These 2 singularities were on the junction part. Nevertheless, the reaction forces were looked at, and all were within acceptable limits. Hotspot results can be found in Table 9.

The restriction is that generic models are used for the textile seatbelts, and the calculations were implicitly made using a simplified generic dummy model representing the human body. While this is acceptable due to the low deformation level and the reaction loads, which are in line with the general loading, a comparison with explicit dynamics, including an actual dummy model, is not necessarily required. Nevertheless, this can be done in future work.

5. Conclusions

The lack of suitable lightweight seats for electrical VTOLs in civil and military applications necessitated this work, where passenger and pilot seats are not distinct. Hence, a troop seat with a textile backrest and seat pan was developed to be safe for emergency landing conditions. The design was made according to military and civilian standards and codes. Loads and boundary

conditions were taken from the maximum values across MIL-S-85510, CS27, and CS29 standards.

There is no distinction between passenger and pilot seats because of the automated systems. Regular pilot seats are too heavy for a weaker electrical powertrain. There are already guiding military standards and civilian codes for physical tests for passenger or pilot seats. Nevertheless, there is no comprehensive document combining all of these. Hence, a generic design was generated based on the troop seat of military helicopters, which was then tested and simulated virtually by finite element analysis according to MIL-S-85510, CS27, and CS29 standards.

In this study, 5 static and 2 dynamic tests were conducted. Mesh sensitivity and hot spot analyses were used to decide whether a design change was required. In the end, all stresses were kept below 10% of the yield strength of the materials. At the same time, targeted weight limitations weren't exceeded. Hence, a near-optimum solution was achieved for electrical VTOL seats after iterations.

To the authors' best knowledge, there were no comparable electrical VTOL seat development examples available in the literature, which is a novel contribution. Existing literature is either for passenger seats or for pilot seats. There is no double-purpose seat proposal for electrical VTOLs. Moreover, the research outlines the simulation methodology and load cases required to develop these VTOL seats by explaining how the results must be interpreted. This is the second contribution to literature, which practitioners can also benefit from.

It has been shown that the structural strength of the troop seat can be increased by using different material combinations, and it was seen that some parts can be thinner to decrease the weight. Also, this research has provided new design recommendations to increase the structural strength of seats. This research offered practical application recommendations for the aviation industry and troop seat manufacturers. Suggestions have been made as to what material combinations or design changes could increase the strength of troop seats without increasing the weight and manufacturing costs. Light weight will also be beneficial for less fuel consumption.

In conclusion, aluminum alloys were appropriate for seat poles and seat pans. Because it was lightweight with high strength. Since high-stress results were observed for the junction part, titanium alloys were more appropriate for use. Because there were no high-stress results for the seat pan, the thickness of the seat pan can be reduced for weight reduction. Instead of using a uniform thickness, the seat pole can be divided into parts with different thicknesses. Because on the middle tube and upper legs of the seat pole, 3 mm thickness was insufficient. Singularity stresses were observed only on the junction part. A detailed joint design and a more detailed dummy model may be used in future studies.

Another future work is conducting accurate tests to verify the analysis results. These simulations can be performed using the Ls-Dyna program, and the results can be compared. In addition to that, the occupant's survivability may be inspected. Fatigue analysis could be conducted as a future study.

CRediT Author Statement

Hasan Totoş: Methodology, Investigation, Data curation, Visualization, Writing-Original Draft, Formal Analysis. **Çağlar Üçler**: Supervision, Conceptualization, Writing – Review and Editing.

Nomenclature

AISI	: American Iron and Steel Institute
Al	: Aluminum
APTA	: American Public Transportation Association
CS27	: Certification Specifications for Small Rotorcraft
CS29	: Certification Specifications for Large Rotorcraft
EASA	: European Aviation Safety Agency
ECE	: European Economic Commission
ETSO	: European Technical Standard Order
eVTOL	: Electrical vertical takeoff and landing
Fe	: Iron
FMVSS	: Federal Motor Vehicle Safety Standards
HS	: Hotspot
MIL-S-85510	: Military specifications for seats, helicopter cabin, crashworthy
MIL-S-58095	: Military specifications for seat system: crash resistant, non-ejection, aircrew
STA	: Solution Treated and Aged
Ti	: Titanium
UAV	: Unmanned air vehicle
USA	: United States of America
V	: Vanadium
VTOL	: Vertical take-off and landing

References

Aldemir, H. O., & Ucler, C. (2022). Airspace deregulation for UAM: Self-organizing VTOLs in metropoles. *The Collegiate Aviation Review International*, 40(1).

Alharasees, O., Jazzar, A., Kale, U., & Rohacs, D. (2023). Aviation communication: the effect of critical factors on the rate of misunderstandings. *Aircraft engineering and aerospace technology*, 95(3), 379-388.

Amaze, C., Kuharat, S., Bég, O. A., Kadir, A., Jouri, W., & Bég, T. A. (2024). Finite element stress analysis and topological optimization of a commercial aircraft seat structure. *European Mechanical Science*, 8(2), 1-17.

Balaban, H. and Penekli, U. (2020). Sonlu elemanlar yöntemlerinin tasarım süreçlerine yararlı etkileri, *Mühendis ve Makina*, 47, 17-22.

Bhavikatti, S. S. (2005). *Finite element analysis*. New Age International.

Bhonge, P. S. (2008). A *methodology for aircraft seat certification by dynamic finite element analysis* (Doctoral dissertation, Wichita State University).

Caccese, V. (2010). Fatigue in laser welds. In *Failure Mechanisms of Advanced Welding Processes* (pp. 218-257). Woodhead Publishing.

Demircan, M. (2020). *Energy Absorber Design and Analysis for Military Utility Helicopter Troop Seats* (Master's thesis, Hacettepe University).

Dinç, A. (2020). Sizing of a Turboprop Engine Powered High Altitude Unmanned Aerial Vehicle and Its Propulsion System for an Assumed Mission Profile in Turkey. *International Journal of Aviation Science and Technology*, 01(01), 9-13.

DoD (1981). MIL-S-85510 (AS) Military Specification Seats, Helicopter Cabin, Crashworthy, General Specification for.

DNV (2011). Fatigue design of offshore steel structures. *Rev.* 3.

EASA (2018). Certification Specifications CS-27: Large Small Rotorcrafts, Amendment 10.

EASA (2018). Certification Specifications CS-29: Large Rotorcrafts, Amendment 11.

Intwala, A., & Parikh, Y. (2015). A review on vertical take off and landing (vtol) vehicles. *International Journal of Innovative Research in Advanced Engineering (IJIRAE)*, 2(2), 187-191.

Ozdemir, U., Aktas, Y. O., Vuruskan, A., Dereli, Y., Tarhan, A. F., Demirbag, K., ... & Inalhan, G. (2014). Design of a commercial hybrid VTOL UAV system. *Journal of Intelligent & Robotic Systems*, 74, 371-393.

Özturk, G., & Kayran, A. (2018). Energy absorption mechanisms and crash analysis of helicopter seats. In ASME *International Mechanical Engineering Congress and Exposition* (Vol. 52040, p. V04BT06A046). American Society of Mechanical Engineers.

Reilly, M. J., & ARMY AIR MOBILITY RESEARCH AND DEVELOPMENT LAB FORT EUSTIS VA EUSTIS DIRECTORATE. (1977). *Crashworthy troop seat testing program* (p. 0206). USAAMRDL-TR-77-13, US Army Research and Technology Laboratories, Ft. Eustis, VA.

Roylance, D. (2001). Finite element analysis. *Department of Materials Science and Engineering, Massachusetts Institute of Technology, Cambridge*.

Trivers, N. C., Carrick, C. A., & Kim, I. Y. (2020). Design optimization of a business aircraft seat considering static and dynamic certification loading and manufacturability. *Structural and Multidisciplinary Optimization*, 62(6), 3457-3476.

Tzanakis, G., Kotzakolios, A., Giannaros, E., & Kostopoulos, V. (2023). Structural Analysis of a Composite Passenger Seat for the Case of an Aircraft Emergency Landing. *Applied Mechanics*, 4(1), 1-19.

Wiggenraad, J. F. M. (1997). Design, Fabrication, Test and Analysis of a Crashworthy Troop Seat, European Rotorcraft Forum.

Zhou, Y., Zhao, H., & Liu, Y. (2020). An evaluative review of the VTOL technologies for unmanned and manned aerial vehicles. *Computer Communications*, 149, 356-369.